Bone regeneration from periosteum and assessment of regenerative bone graft into the bone defect

Takayuki Mashimo

Nihon University Graduate School of Dentistry,

Major in Oral and Maxillofacial Surgery

(Director: Prof. Yoshiyuki Yonehara)

Table of Contents

The following two articles are part of this doctoral dissertation:

Journal of Hard Tissue Biology, 22(4): 391-400, 2013

Journal of Hard Tissue Biology (in press)

Abstract

In maxillofacial bone defects caused by trauma and tumor resection, autogenous bone graft is indispensable for reconstruction to improve QOL of the patients in post-operation. However, autogenous bone graft is involved in the variety of factors such as donor-site morbidity and bone volume used as a transplant. Bone-like materials have been developed to overcome these problems, but they cannot completely exclude pathological problem including foreign-body reaction. Since periosteum has a potential to induce bone formation through osteoblast differentiation, the experiments in this study were to demonstrate the usefulness of periosteum-induced bone as a new graft material for the maxillofacial reconstruction.

In the first chapter, bone regenerative effect of periosteum with blood supply was examined in rat hind limb which fibula was excised. Micro-CT analysis showed that regenerating fibula in the periosteum appeared first in the center of diaphysis at 5 day, and extended gradually to epiphysis until 8 weeks. No bone regeneration was found in the lack of periosteum, even 8 weeks passed. Histologically, periosteum-induced bone of fibula was immature woven bone at 1 week, formation of lamellar bone at 4 week, and mature bone at 8 week. However, quantitative analysis showed that periosteum-induced bone was different from normal bone, because its diameter was thick in the early stage and gradually became thinner as is the case of healing of bone fracture.

In the second chapter, periosteum-induced bones regenerated after removal of fibula were transplanted at 1, 4 and 8 weeks into the bone defect prepared experimentally in the inferior margin of mandible. The engrafted bone was examined at 2 and 4 weeks. Micro-CT and histological analyses showed that engrafted bones were completely integrated in the native mandible, resulting in restoration of the defects, but some histological differences were observed depending on the maturity of bone. In the case of immature bone transplant, marrow-cell rich bones with low density and few numbers of osteoclasts were observed in engrafted bone. In contrast, high-density bony tissues with a large number of active osteoclasts were defined, when mature bones were transplanted.

Taking together, these results suggest that periosteum-induced bone in fibula is suitable for the restoration of bone defects in mandible. However, there is the problem that maturity of engrafted bones affects bone density and the number of osteoclasts in restorative bone tissues. Therefore, the timing when periosteum-induced bone is collected from donor site would be critical for the better bone graft in the recipient site.

Chapter 1: Assessment of the Bone Regenerative Process from Fibular Periosteum by *in vivo* Micro Computed Tomography

Takayuki Mashimo, Tadahito Saito, Hiroshi Shiratsuchi, Jun Iwata, Takeshi Uryu, Takaaki Tamagawa, Shunsuke Namaki, Kunihito Matsumoto, Shouji Kawashima,Yoshiyuki Mori, Yoshinori Arai, Kazuya Honda, Yoshiyuki Yonehara

Journal of Hard Tissue Biology, 22(4): 391-400, 2013

Introduction

Maxillofacial bone defects resulting from tooth extraction, trauma, or tumor resection have been repaired with autogenous bone grafts or artificial materials. Autogenous bone grafting is generally an effective technique, but has disadvantages such as donor-site morbidity. Artificial materials have been developed to overcome the disadvantages of autogenous bone grafts, but can cause adverse effects such as foreign-body reactions. Since both autogenous bone grafts and artificial materials have inherent advantages and disadvantages, it is necessary to develop new reconstruction materials. This study has focused on the use of periosteum as a new material with low morbidity and no foreign-body reactions. The use of bone regenerated from periosteal grafts is considered clinically significant.

The periosteum is a connective tissue that covers the surface of bone. This tissue consists of two layers, a thick outer fibrous layer and an inner osteogenic layer (cambium layer) [1]. The cambium layer plays an important role in osteogenesis. The osteogenic capacity of periosteum was first reported by Duhamel et al.[2] in 1739. However, stable results with free periosteum grafts were not obtained in experimental studies, and the osteogenic potential of periosteum remained controversial[3-5]. Clinically, Skoog[6,7] introduced the use of maxillary periosteal flaps for primary repair of alveolar clefts in the 1960s. Ritisila et al.[8] used free periosteal grafts from the tibia for primary repair of the palate. These reports restimulated interest in the osteogenic capacity of periosteum. Several studies reported that vascularized periosteum has good osteogenic properties, suggesting that vascularity has an important role in periosteum-related osteogenesis[9-12]. In addition, Acland and van den Wildenberg et al.[13,14] reported that mechanical stress influences the osteogenic capacity of periosteum. Takato et al.[15,16] found that the osteogenic capacity of periosteum depends not only on weight and stress, but also on the volume of periosteum and the blood circulation. Uddströmer et al.[17,18] demonstrated that periosteum is intimately involved in fracture healing. Oni et al.[19,20] found that removing the periosteum prevents fracture healing. Li et al.[21] showed that cartilaginous and osteoid bone derived from periosteum participate in fracture healing. Thus, the periosteum has been reported to have osteogenic potential, but the bone regenerative process

from periosteum, including the time course of osteogenesis, regenerative bone volume and bone mineral density, remains poorly understood.

Vascularized fibula grafting has been shown to be an effective technique for reconstruction of the maxillofacial region[22,23]. However, the disadvantages of this technique are restricted availability of suitable grafts and high invasion associated with acquiring bone from donor sites. If regenerative bone from fibular periosteum could be used in place of direct bone grafts, it would be possible to reconstruct jaw bones without directly using the fibula.

A better understanding of the timing and properties of regenerative bone from periosteum may provide important clues to the optimal timing of periosteal grafting. Recently, most studies of periosteum examined the repair process in segmental bone defect models and bone fracture models[24-27]. Few studies have focused exclusively on fibular periosteum. Studies examining the details of bone regeneration from periosteum in the same subjects are extremely rare.

A recently developed micro-computed tomography (micro-CT) system, R_mCT® (Rigaku Co., Tokyo Japan), has made it possible to obtain images of anesthetized experimental animals. Clear hard tissue images of small animals can be obtained with short exposure time and low dose. A lot of studies have proven the value of micro-CT for the assessment of changes over time in the animal experiments[28,29]. Saito et al.[30] have concluded that micro-CT is suitable for evaluating bone regenerative process after mandibular condylectomy in rat model and periosteum plays a critical role in bone regeneration of mandibular condyle. However, the detail of regenerative process of long bones such as fibula is unclear. Thus, this study conducted the assessment of the detailed process of bone regeneration from fibular periosteum of experimental animals over time using micro CT.

Materials & Methods

Animals

Twenty 6-week-old male Wistar rats with a mean body weight of 130 g (Sankyo Laboratory, Tokyo, Japan) were used in the study. The rats were divided into two groups: a periosteum preservation (PP) group (n=15) and a periosteum removal (PR) group (n=5). The animals were housed in an experimental animal room (22°C, 55% relative humidity, and a 12-h light/dark cycle) and fed a standard laboratory diet. Water was provided ad libitum. The Animal Experimentation Committee of the Nihon University School of Dentistry approved this study.

Sargical Procedure

All surgical procedures were performed with the animals under intraperitoneal anesthesia with sodium pentobarbital (50 mg/kg body weight; Somnopentyl, Schering-Plough, Munich, Germany). The surgical site was shaved, and the skin was washed with 70% ethanol. The site was then locally anesthetized with an intramuscular injection of 1 ml 2% lidocaine (Xylocaine, Astra-Zeneca, Osaka, Japan). A lateral skin incision about 20 mm in length was made in the lower leg, and a smaller incision was made into the gastrocnemius muscle. The muscle was retracted to expose the connections of the tibia and fibula. An osteotomy was performed at the epiphysis of the fibula. In the PP group, the gastrocnemius muscle and periosteum were detached from the fibular diaphysis, and the fibula was totally removed by pulling peripherally with the use of surgical clips; the blood supply to the periosteum was maintained (Fig. 1-A, B, C). In the PR group, the same procedure was performed; however, the periosteum was not detached and removed with the fibula (Fig. 1-D). After the fibula was removed, the muscle and skin were closed with 5-0 nylon sutures (Bear Medic Co., Tokyo, Japan). Rats were sacrificed at 5 days and 1, 2, 4, 6, and 8 weeks after operation.

Radiographic analysis

Before operation, immediately after operation, and 3 days, 5 days, and 1, 2, 4, 6, and 8 weeks after operation, the bone-defect region underwent radiographic analysis by in vivo micro computed tomography system (R_mCT; Rigaku Co., Tokyo, Japan). Longitudinal, cross-sectional, and 3-dimensional images (3D images) were examined. During exposure, the rats were anesthetized with isoflurane (DS Pharma Animal Health Co. Ltd., Osaka, Japan). The exposure conditions were 17 seconds at 90 kv/100 mA. The image volume was a cylinder 2.4 cm in diameter and 2.4 cm high with a voxel matrix size set to 481 × 481 × 483. The longest lengths and diameters of regenerative bone were measured in millimeters (mm) with the use of image reconstruction software (i-VIEW-R; Morita Co., Kyoto, Japan) (Fig. 2-A, B).

Quantitative analysis

The bone volume and bone mineral density of the whole regenerative bone were measured in cubic millimeters (mm^3) and milligrams per cubic centimeter (mg/cm^3) with the use of quantitative analysis software (3-by-4 viewer 2011, Kitasenju Radist Dent, Tokyo, Japan) (Fig. 2-C).

Statistical analysis

These data expressed as the mean ± SD for each group. Statistical differences were analyzed using Scheffe's test. Values of $P < 0.05$ were considered statistically significant.

Histological analysis

Five days and 1, 2, 4, 6, and 8 weeks after surgery, regenerative bone was extirpated and fixed in 4% paraformaldehyde phosphate buffer solution. The resected specimens were decalcified in 10% EDTA (Dojindo, Kumamoto, Japan) for 10 days at 4°C. The specimens were then dehydrated in a graded series of ethanol, embedded in paraffin, and sectioned transversely at a thickness of 8 μm. The sections were stained with hematoxylin and eosin. Chondrocyte were identified by alcian bule staining, and osteoclasts were identified by tartrate-resistant acidic phosphate (TRAP) staining using a TRAP/ALP stain kit (Wako, Tokyo, Japan). Histologic examination was performed under a light microscope equipped with a morphometric system connected to a personal computer.

Results

Radiographic analysis

Regenerative bone on the fibula was examined using micro computed tomography and was quantified with reconstruction software (i-VIEW) in cross-sectional and longitudinal planes. Immediately after operation, both groups showed that the fibula had been totally removed (Fig. 3, 4). The CT images of the PP groups showed initial signs of bone formation on the fibula 5 days after operation (Fig. 3-A, B, C, arrow). Bone regeneration began at the center of the diaphysis and gradually progressed to the epiphysis (Fig. 3-A, C). Three-dimensional images of regenerative bone showed that the bone surface was rough at 5 days and 1 week, but then gradually became smooth up to 8 weeks (Fig. 3-C). Morphometric analysis of CT image slices showed that the length of regenerative bone on longitudinal images continued to increase gradually until 8 weeks (Fig. 5, Table). The diameter of regenerative bone on cross-sectional images was thickest at 1 week, but then gradually decreased until 8 weeks (Fig. 6, Table). At the knee joint, epiphyseal cartilage had increased (Fig. 3-C, arrowhead), but this tissue was not studied because it was not bone regenerated from fibular periosteum, but tissue regenerated from the stump of cartilage. In the PR group, the stump of the fibula at the knee joint increased (Fig. 4-C, arrowhead), but there was not bone regeneration at the center of the diaphysis up to 8 weeks (Fig. 4-C).

Quantitative analysis

Quantitative analysis of bone regeneration on the fibula was performed with analysis software (3-by-4 viewer 2011) to estimate regenerative bone volume and bone mineral density (Fig. 2-C). In the PP group, regenerative bone volume increased remarkably at 1 week, but decreased at 2 weeks. After 2 weeks the bone volume increased slightly up to 4 weeks, but there was little change thereafter (Fig. 7, Table 1). In contrast, regenerative bone mineral density continued to increase gradually up to 6 weeks. There was little change after 6 weeks (Fig. 7, Table 1). In the PR group, there was no evidence of regenerative bone during the 8 weeks of observation.

Histological analysis

In the PP group, woven bone surrounded by periosteum (Fig. 9-A, black arrow) emerged at the center of regenerative bone at 5 days (Fig. 9-A, yellow asterisks) and was present until 2 weeks (Fig. 9-B, C, yellow asterisks). During 2 to 4 weeks, the woven bone changed to lamellar bone (Fig. 9-D, green asterisks). After 4 weeks, there were no significant changes in the histological findings (Fig. 9-D, E, F). At the epiphysis of regenerative bone, cartilage-like tissue was observed at 5 days (Fig. 10-A, B, black asterisk). The cartilage-like tissue was stained with alcian blue. In addition, at the diaphysis of that, $TRAP^+$ osteoclasts were observed inside the regenerative bone at 5 days and 1 week (Fig. 11-A, B, black arrowhead). At 2 weeks and 4 weeks, $TRAP^+$ osteoclasts were observed not only inside the bone, but also around the bone (Fig. 11-C, D, black arrowhead). At 6 weeks and 8 weeks, $TRAP^+$ osteoclasts were observed only around the bone (Fig. 11-E, F, black arrowhead).

Discussion

The present study showed that when the fibula was totally removed, and the periosteum and its blood supply were preserved (PP group), bone formation was evident. However, when the fibula was removed including the periosteum (PR group), there was no bone formation at all. These results suggest that the periosteum has osteogenic capacity. As mentioned above, many investigators have reported the osteogenic capacity of the periosteum [1-18]. Bone regeneration from the periosteum was found to depend on mechanical stress and blood supply [16,17]. However, the most important events in bone formation occur at the cellular level. Recent studies have demonstrated that progenitor cells, such as mesenchymal stem cells (MSCs), exist inside the periosteum, especially in the inner cambium layer[31,32]. Such MSCs can form bone in vitro and in vivo[33,34]. MSCs derived from periosteum have a greater osteogenic potential in vitro than those derived from other local tissues, such as adipose tissue

or synovium.[35)]

The PP group showed obvious bone formation, whereas the PR group showed no bone formation. The reason for the difference between the groups was attributed to the presence of MSCs. However, this study could not identify the existence of MSCs in periosteum, because marker proteins expressed by MSCs, such as CD29, CD90, and CD105[36)] were not found. Further research is needed on the detection of MSCs by immunohistochemical staining.

In the present study, the time course of bone regeneration was followed in the same subjects. The regenerative bone at defects was examined in detail by means of in vivo micro CT. Micro CT showed that bone formation began at the center of the diaphysis and gradually progressed to the epiphysis in the PP group. Morphometric analysis revealed that the regenerative bone tended to change into long and narrow bone. These changes in the bone appeared to be due to the fibular periosteum promoting extension and growth of the tibia and gastrocnemius muscle. With the use of analysis software, it was possible to quantitatively assess regenerative bone. In the PP group, bone volume clearly increased until 1 week, but then decreased at 2 weeks. After 2 weeks, the bone volume gradually tended to increase again until 8 weeks. However, there was no obvious difference between 4 and 8 weeks. The bone mineral density continued to increase until 6 weeks, although there was no apparent difference between 6 and 8 weeks. Three-dimensional images of regenerative bone showed that the bone surface was rough at 5 days and 1 week, but then gradually became smooth up to 8 weeks. In addition, HE staining of the sections showed that regenerative bone from periosteum was initially observed as woven bone at the epiphysis at 5 days. The woven bone gradually changed to lamellar bone up to 8 weeks. There were no significant histological changes from 4 to 8 weeks. These findings showed that immature bone was replaced by mature bone throughout bone remodeling. Remodeling is responsible for changes in bone shape and mass to renew bone, associated with the presence of osteoblasts and osteoclasts[37)]. In this study, TRAP staining to detect the localization of osteoclasts was performed. Localization of $TRAP^+$ osteoclasts changed with time. $TRAP^+$ osteoclasts were found only inside woven bone at 5 days to 1 week, inside and around bone at 2 to 4 weeks, and only around lamellar bone at 6 to 8 weeks. These results suggest that remodeling occurs within regenerative bone at an early stage, and the site of the remodeling shifts to the bone surface with bone mature at the final stage. Remodeling of mature bone is generally thought to occur at the cortical bone surface[37)]. Therefore, this study demonstrated the mature process of regenerative bone during 8 weeks. This study suggested that the development of mature regenerative bone from periosteum was completed at 4 to 6 weeks.

Most previous studies using fibular periosteum examined the repair of segmental bone

defects as a model of fracture healing[19-21]. These studies showed that bone repair involves ossification in the fracture gap and subperiosteal direct bone formation over cortical bone[24,25]. These previous investigations examined the mechanism of bone fracture healing and did not focus only on the function of the periosteum. Another purpose of these studies of fibular defects was to observe bone regeneration using particulate artificial bone, cells, and biomaterials[26,27]. The results focused on conditions associated with the formation of more regenerative bone. To my knowledge, no previous study used a model lacking fibula in which the blood supply to the periosteum was maintained to directly investigate the periosteal function. The PP model used specifically allowed assessment of the functions of fibular periosteum for the first time. However, the process of bone regeneration in this model was similar to that previously reported in segmental bone defects[24-27]. These regenerative bone in previous reports were thick in the early stage, but gradually became thinner during processes such as fracture healing[38]. In previous study, a similar process was observed in a temporomandibular joint defect model in which the periosteum was maintained[35]. It is interesting to note that the process of bone regeneration from only periosteum was associated with a transient decrease in bone volume. This phenomenon can be explained by the mechanism of bone-fracture healing. After fracture, a hematoma forms beneath the periosteum, and the hematoma is replaced by callus bone, which has a woven structure. The bone undergoes repeated resorption and formation by remodeling and changes to lamellar bone. Consequently, repaired bone becomes thin and functional[38]. These processes underlie bone regeneration in the PP model. Since nearly all previous studies reported that rat fibular defects were repaired in 4 to 8 weeks[24,26,27], this study suggests that the regenerative process described in past reports followed a similar course as bone regenerated from only periosteum.

Another similarity with previous studies was the ossification pattern of bone regenerated from fibular periosteum. Periosteum of long bones such as the tibia and fibula has osteogenic capacity due to endochondral ossification, while that of membrane bones such as the calvaria has osteogenic capacity due to membranous ossification[39]. Therefore, regenerative bone in this study would be formed by endochondral ossification because this model used fibular periosteum. Endochondral ossification is a process in which bone replaces cartilage. In this type of ossification, formed cartilage is replaced by bone from the central part, and replacement of cartilage by bone then proceeds longitudinally[39]. Radio-opacity images at 5 days indicated where bone replaced cartilage, but could not identify cartilage tissue. However, histological examination at 5 days showed the presence of woven bone at the center of regenerative bone, but cartilage tissue at the epiphysis. This cartilage tissue indicated the top of the epiphysis during endochondral ossification. Thus, this study demonstrated that bone regenerated from fibular periosteum was formed by endochondral ossification.

Clinically, there appear to be two methods to promote the formation of regenerative bone from periosteum. The first method is to induce the formation of regenerative bone by securing a space between bone and periosteum at the donor site. The second method is to form bone at the recipient site by grafting vascularized periosteum. Thus, if bone regenerated from fibular periosteum can be used for bone grafts, it is possible to reconstruct the jawbone without using the fibula itself. These results are promising because they showed that the properties of regenerative bone depend on the observation period. The volume of bone derived from periosteum was greatest at 1 week, but the bone was immature. At 4-8 weeks, the bone was more mature than that at 1 week with respect to bone mineral density and histological characteristics. This study shows that it is necessary to determine the optimal timing of grafting. Future studies are required to investigate whether bone regenerated from fibular periosteum can be used for bone grafts and to define the optimal timing for grafting and the conditions that most efficiently promote the formation of bone regenerated from periosteum.

Chapter 2: A New Graft Material for Mandibular Bone Defect Repair Using Regenerative Bone from Periosteum.

Takayuki Mashimo, Tadahito Saito, Hiroshi Shiratsuchi, Jun Iwata, Takeshi Uryu, Takaaki Tamagawa, Tomohiro Yasumitsu, Shunsuke Namaki, Kunihito Matsumoto, Yoshiyuki Mori, Yoshinori Arai, Kazuya Honda, Yoshiyuki Yonehara

Journal of Hard Tissue Biology (in press)

Introduction

The repair of bone defects caused by tumor resection, traumatic loss, and jaw cysts remains an unsolved problem. Autogeneous bone grafts or artificial materials can be used, but each has advantages and disadvantages. The use of autogeneous bone grafts has become a well-accepted procedure for the restoration of the function and structure of the jaw. However, autogeneous bone grafts are limited in supply and can cause clinically significant donor-site morbidity. Although artificial materials have been used clinically, bone regeneration is not superior to that obtained with autogeneous bone grafts.

To develop new materials, The function of periosteum as a new reconstructive material, which is associated with relatively low morbidity, was evaluated previously[30,40]. Several studies have demonstrated that vascularized periosteal grafts have excellent osteogenic capacity and promote the formation of bone in bone defects[6,10,41,42]. A recent study reported that cultured periosteum-derived cells show osteogenic capacity in bone defects[43]. Although many investigators have suggested that periosteum can be used as a reconstructive material, no study has used regenerative bone from periosteum as a graft.

This study planned a series of experiments to transplant regenerative bone from periosteum into bone defects. As a pilot study, the details of bone regeneration from fibular periosteum, including the time course of bone regeneration, bone volume, and bone mineral density (BMD) by means of micro-computed tomography (CT) were investigated[40]. The results showed that the properties of regenerative bone differed according to the time course. The present study was designed to evaluate the optimum timing for grafting regenerative bone from periosteum. Regenerative bones harvested from fibular periosteum at different times were transplaned into rat mandibular defects and the bone-graft regions were assessed.

Materials and Methods

Animals

Twenty-four Wistar male rats (body weight: 130 g, Sankyo Laboratory, Tokyo, Japan) were used as donor and recipient animals in this study. Eight rats were used as donor rats, and 16 were used as recipient rats. The animals were housed in an experimental room (22°C, 55%, humidity, and 12-h light/dark cycle) and fed a standard laboratory diet and water. The Animal Experimentation Committee of the Nihon University School of Dentistry approved this study (AP10D020). The experimental protocol is shown in Fig. 12.

Harvesting of regenerative bone from periosteum as grafts

A previously established protocol was used[40]. All surgical procedures were performed with the experimental animals under intraperitoneal anesthesia with pentobarbital sodium (50 mg/kg, body weight; Somnopentyl, Schering-Plough, Munich, Germany). The right and left fibulas were totally removed from 6 donor rats, preserving the periosteum. After removing the fibulas, 2 rats each were sacrificed with an overdose of pentobarbital at 1, 4, and 8 weeks, respectively, and the regenerative bones were harvested as grafts. Two other rats in which the fibulas were not removed were sacrificed, and the fibulas were harvested as normal fibula grafts. The graft bones were trimmed to the size of 1 × 5 mm (Fig. 13).

Transplantation of graft bones into the mandibular defect of recipient rats

Recipient rats were divided into 4 groups: a normal fibula (NF) transplantation group (NF group), a regenerative bone at 1 week (RB1) transplantation group (RB1 group), a regenerative bone at 4 weeks (RB4) group (RB4 group), and a regenerative bone at 8 weeks (RB8) group (RB8 group). After anesthetization, the skin at the surgical region was shaved and disinfected, and a full-thickness skin incision was made along the inferior border of the left side of the mandible. The masseter muscle and the periosteum covering the buccal surface of the mandible were elevated as a flap. A bone defect (1×5 mm) was made using a diamond disk (φ = 5 mm) with copious saline irrigation in the inferior border of the mandible (Fig. 14A). The bone defect region was debrided with saline, and each graft bone (NF, RB1, RB4, and RB8) was transplanted into the defect of each recipient rat (NF groups, RB1 groups, RB4 groups, and RB8 groups) (Fig. 14B). After transplantation, the masseter muscle was repositioned and sutured, and the skin incision was closed with 5-0 nylon thread. Surgery was performed in 16 rats, and the 4 types of graft bone were transplanted into 4 rats each.

Micro-CT examinations

All 16 rats underwent in vivo micro-CT using R_mCT® system (Rigaku Co., Tokyo, Japan) immediately, 2, and 4 weeks after transplantation. During exposure, the rats were anesthetized with isoflurane (DS Pharma Animal Health Co. Ltd., Osaka, Japan). The exposure conditions were 17 seconds at 90 kv/100 mA. The image volume was a cylinder 2.4 cm in diameter and 2.4 cm high, with a voxel matrix size set to 481 × 481 × 483.

Micro-CT image analysis

Immediately and 4 weeks after transplantation, the height and width of the mandible were measured with the use of image reconstruction software (i-VIEW-R; Morita Co., Kyoto, Japan). The measurement area was determined on the coronal plane, in the region of the foramen mandibulae. The height of the mandible immediately after making the defect was calculated with a length tool, from the lower border of the foramen mandibulae to the lower border of the defect, in millimeters (Fig. 15A-1). The height at 4 weeks after transplantation was calculated from the lower border of the foramen mandibulae to the inferior border of the mandible, in millimeters (Fig. 15A-2). The length tool was used to calculate the width of the lower border of the mandible immediately after making the defect and 4 weeks after transplantation, in millimeters and in the same area, on the coronal plane (Fig. 15B-1, B-2). The ratio between the length (height and width) 4 weeks after transplantation and that immediately after making the defect was used as the measurement. In addition, the BMD of the inferior border of the newly formed mandible after 4 weeks, which was contained in a defined rectangle, was calculated in milligrams per cubic centimeter (mg/cm^3) with the use of quantitative analysis software (3-by-4 viewer 2011, Kitasenju Radist Dent, Tokyo, Japan). The defined rectangle (2 × 2 × 2 mm) was evaluated on coronal, sagittal, and axial planes, using the region of the foramen mandibulae as a guide (Fig. 16).

Statistical analysis

Means and standard deviations were calculated for the height ratio, width ratio, and BMD. Statistical differences were analyzed using the Mann-Whitney test. Values of $P < 0.05$ were considered to indicate statistical significance.

Histological analysis

After 4 weeks, rats in each group were sacrificed, and the left side of the mandible was resected and fixed in 4% paraformaldehyde phosphate buffer solution. The resected specimens were decalcified in 10% EDTA (Dojindo, Kumamoto, Japan) for 10 days at 4°C. The specimens were then dehydrated in a graded series of ethanol, embedded in paraffin, and

sectioned transversely at a thickness of 8 μm. The sections were stained with hematoxylin and eosin. The osteoclasts were identified by tartrate-resistant acidic phosphate (TRAP) staining, using a TRAP/ALP stain kit (Wako, Tokyo, Japan). Histological analysis was performed under a light microscope equipped with a morphometric system connected to a personal computer.

Results

Clinical evaluation

Wound healing was uneventful, with limited signs of inflammation. Four weeks after transplantation, the wounds in all groups remained closed, without any sign of graft exposure during the healing period.

Micro-CT examinations

To evaluate the morphology of the mandible after transplantation of the bone grafts, micro-CT was taken immediately, 2 weeks, and 4 weeks after transplantation. Representative images (three-dimensional and coronal planes) from each group are shown in Fig. 17. Immediately after transplantation, the bone grafts were observed in the mandibular defects in all groups (Fig. 17, arrowheads). After 2 weeks, bony connections were observed between the bone grafts and native bone tissue in all graft groups, but the NF, RB4, and RB8 groups showed a trend toward resorption of the grafted bone at the inferior border of the mandible (Fig. 17, arrows). In contrast, the RB1 group showed no signs of resorption of the grafted bone. After 4 weeks, the degree of resorption of the grafted bone at the border of the mandible was slightly greater than that at 2 weeks, but resorption in the RB1 group appeared to be less than that in the other groups.

Micro-CT image analysis

To quantify the bone grafts after transplantation, the height and width of the mandible and the BMD of the mandibular border were calculated with the use of two types of software. The mean height ratios are shown in Fig. 18. The height ratio in the RB1 groups was significantly higher than that in the NF groups ($P < 0.05$). In contrast, the height ratio in the RB8 groups was significantly less than that in the NF groups ($P < 0.05$). The height ratio did not differ significantly between the NF and RB4 groups ($P > 0.05$). The mean width ratios are shown in Fig. 19. The width ratio in the RB1 groups was significantly higher than that in the NF groups ($P < 0.05$). The width ratios were similar in the NF, RB4, and RB8 groups ($P > 0.05$). The mean BMD is shown in Fig. 20. BMD in the RB1 groups was significantly less

than that in the NF groups ($P < 0.05$). BMD was similar in the NF, RB4, and RB8 groups ($P > 0.05$).

Histological analysis

The graft sites of the mandible after HE and TRAP staining are shown in Fig. 21. After 4 weeks, bone healing was observed in the 4 specimens. It was difficult to discern differences in the defect edge, graft bone, and newly formed bone (Fig. 21, blue dotted lines). In the NF groups, lamellar bone and bone marrow were seen at the inferior border of the mandible. The surface of bone was smooth. $TRAP^+$ osteoclasts (Fig. 21, black arrowheads) were found on the bone surface and within the bone marrow (Fig. 21, black asterisks). In the RB1 groups, the inferior border of the mandible was characterized by lamellar bone and a large amount of bone marrow. The bone surface was smooth. $TRAP^+$ osteoclasts were found on the bone surface and within the bone marrow. The RB4 groups showed lamellar bone with little bone marrow. The bone surface was smooth. $TRAP^+$ osteoclasts were found on the bone surface. In the RB8 groups, lamellar bone similar to that in the RB4 groups was found, but the bone surface was rough and showed signs of resorption. A large number of $TRAP^+$ osteoclasts were found on the bone surface.

Discussion

In this study using regenerative bone from periosteum and a rat mandibular defect model, regenerative bone grafts were completely integrated into the native bone tissue without infection and achieved repair of the mandibular defect. However, some differences in the repair process were found among all of the graft groups.

The first point to be discussed is the morphological and qualitative differences in the bone grafts after transplantation. Morphological analysis revealed that the height and width ratios in the RB1 groups were significantly higher than those in the NF groups, and the height ratio in the RB8 groups was significantly less than that in the NF groups. Qualitative analysis revealed several architectural changes in bone. BMD in the RB1 groups was significantly less than that in the NF groups, because the RB1 groups had a larger amount of bone marrow than the NF groups on histological images. BMD was similar in the NF, RB4, and RB8 groups, but histological examination showed some differences. More $TRAP^+$ osteoclasts were found on the bone surface in the RB8 groups than in the NF groups. These results suggested that RB1 resists resorption and has higher regenerative potential than NF, whereas the properties of RB4 appear to be similar to those of NF, and RB8 seemed to be resorbed faster than NF. Thus, the present study suggests that the properties of regenerative bone from periosteum differ

considerably, depending on the timing of transplantation.

A previous study investigated the properties of regenerative bone from the fibular periosteum used in this study[40]. Previous results showed that regenerative bone at 1 week was juvenile bone with a large amount of bone marrow, regenerative bone at 4 weeks was bone immediately after becoming mature, and regenerative bone at 8 weeks was completely mature. On comparing the present results with those of a previous study, juvenile bone grafts such as RB1 resisted resorption and had high regenerative activity as compared with mature bone grafts such as RB8.

It is generally believed that grafted bone tends to be resorbed after connecting with the native bone. Previously, many investigators have studied the resorption of various graft bones after transplantation[44-48]. Iwata et al.[47,48] evaluated fetal bone as material for graft bone. They suggested that fetal bone had higher growth potential than mature bone and was useful as a graft material. Attempts to graft fetal tissue were started in the 1970s. First, fetal small intestines[49] and fetal kidneys[50] were used for grafting on an experimental basis. In addition, fetal hepatocytes[51] and thymuses[52] were used clinically to treat severe combined immunodeficiency disease (SCID). Parkinson's disease has been successfully treated clinically, using fetal adrenal cells[53] or nerve cells[54]. Because fetal tissue grafts have high potential for growth and differentiation, it has been reported that they can be used as donor tissue[55].

These previous findings are consistent with the results of the present study. RB1 is juvenile bone similar to fetal bone. As RB1 has high potential for growth and differentiation, it resisted resorption and had high regenerative ability as compared with NF. In contrast, RB4 and RB8 are mature bone and have lower potential for growth and differentiation than RB1. In particular, RB8, which is completely matured bone, tended to be resorbed faster than RB4. These findings indicate that regenerative bone from periosteum at an early time had higher reproductive ability as graft bone than did regenerative mature bone.

Next, the clinical significance of this study should be discussed. Clinically, autogeneous bone grafts are considered the gold standard for repair and reconstruction of bone[56,57]. Vascularized fibula grafting has been shown to be an effective technique for reconstruction of the maxillofacial region[22,23]. However, the disadvantages of autogeneous bone grafts are restricted availability of suitable grafts and high invasion associated with acquiring bone from donor sites. Although many investigators have evaluated the possibility of using periosteum as a reconstructive material which is associated with relatively low morbidity[6,10,41,42], studies using regenerative bone from periosteum as grafts have yet to be reported. The present study is the first report to document the use of regenerative bone from

periosteum as grafts. If regenerative bone from fibular periosteum could be used as a graft bone, it would be possible to reconstruct the jaw without using fibula bone. Therefore, this study assumes that there are two methods to use regenerative bone from periosteum as graft bone clinically. The first method is to induce the formation of regenerative bone by securing a space between bone and periosteum at the donor site, and the formed bone in the space is used as a graft bone. The second method is to transplant harvested periosteum into the muscle, and the formed bone in the muscle is used as a graft. In particular, the second methods may induce the regenerative bone formation, which is appropriate to recipient shape, by the form of transplanted periosteum. Thus, if the regenerative bone in the body could be used, it is suggested that this is clinically significant.

These results suggest that the optimal timing of regenerative bone grafts should be altered depending on the bone volume or quality required at a given recipient site. If a large amount of bone volume is required clinically, juvenile bone such as RB1 is appropriate for transplantation. If high-density, hard bone is required, mature bone such as RB4, which is similar to normal bone, is appropriate for transplantation, whereas completely mature bone such as RB8 is not appropriate for transplantation.

Several investigators have compared membranous bone grafts with endochondral bone grafts[58,59]. They hypothesized that endochondral bone grafts are resorbed faster than membranous bone grafts, because endochondral bone grafts had a greater proportion of cancellous bone, which was revascularized more quickly and was subject to osteoclastic resorption. Osteogenic activity has been reported to differ between membranous bone and endochondral bone, and the ossification of regenerative bone from periosteum depended on the ossification of original bone[39]. In the present study, regenerative bone from periosteum of the fibula, which is endochondral bone, was investigated. Further studies are needed to evaluate regenerative bone from membranous bone periosteum, such as calvarial periosteum, and to apply the regenerative bone graft clinically.

Conclusions

To demonstrate the usefulness of periosteum as a new bone graft material, the regenerative activity of periosteum and restorative ability of periosteum-induced bone were investigated in experimental models of rat. The following conclusions were obtained.

1. Fibular periosteum has osteogenic capacity and the peak of bone regeneration from the periosteum occurs around 4 to 6 weeks.
2. Periosteum-induced bone of fubula restores the bone defect experimentally prepared in the inferior margin of mandible.
3. Maturity of engrafted bone affects bone density and bone resorption in restorative bone tissues.

Collectively, it is clearly demonstrated that periosteum-induced bone is suitable for a bone graft material in maxillofacial reconstruction, but the timing when periosteum-induced bone is harvested from donor site would be critical for the better bone graft in the recipient site.

Acknowledgments

This work was supported in part by Grants-in-Aid for Scientific Research (24593063) from the Japan Society for the Promotion of Science (JSPS), Grants from the Dental Research Center, Sato Funds, Uemura Fund of Nihon University School of Dentistry, as well as special research grants for the development of distinctive education for private schools of Japan.

References

1. Canalis RF, Burnstein FD (1985) Osteogenesis in vascularized periosteum. Arch Otolaryngol 111: 511-513.

2. Duhamel H.L (1739) Observations de physique generale. Histoire de L'Academie Royale desSciences. De L' imprimerie Royale: 1-3.

3. Mc Williams C.A (1914) The function of the periosteum in bone transplants, based on four human transplantations without periosteum, and some animal experiments. Surg Gynec Obstet 18: 158-169.

4. Phemister D.B (1914) The fate of transplanted bone and regenerative power of its various constitunents. Surg Gynec Obstet 19: 303-333.

5. Davis JS, Hunnicutt JA (1915) The osteogenic power of periosteum: with a note on bone transplantation, An experimental study. Ann Surg 61: 672-685.

6. Skoog T (1967) The use of periosteum and Surgicel for bone restoration in congenital clefts of the maxilla: a clinical report and experimental investigation. Scand J Plast Reconstr Surg 1: 113-130.

7. Skoog T (1969) Repair of unilateral cleft lip deformity: maxilla, nose and lip. Scand J Plast Reconstr Surg 3: 109-133.

8. Ritsila V, Alhopuro S, Gylling U, Rintala A (1972) The use of periosteum for bone formation in congenital clefts of the maxilla: a clinical report. Scand J Plast Reconstr Surg 6: 57-60.

9. King KF (1976) Periosteal pedicle grafting in dogs. J Bone Joint Surg Br 58: 117-121.

10. Finley JM, Acland RD, Wood MB (1970) Revascularized periosteal grafts a new bone without bone grafting. Plast Reconstr Surg 61: 1-6.

11. Buncke HJ, Furnas DW, Gordon L, Achauer BM (1977) Free osteocutaneous flap from a rib to the tibia. Plast Reconstr Surg 59: 799-804.

12. Puckett CL, Hurvitz JS, Metzler MH, Silver D (1979) Bone formation by revascularized periosteal and bone grafts, compared with traditional bone grafts. Plast Reconstr Surg 64: 361-365.

13. Acland RD (1978) Caution about clinical use of vascularized periosteal grafts. Plast Reconstr Surg 62: 290.

14. van den Wilderberg FA, Goris RJ, Tutein Nolthenius-Puylaert MB (1984). Free revascularised periosteum transplantation: an experimental study. Br J Plast Surg 37: 226-235.

15. Takato T, Harii K, Nakatsuka T, Ueda K, Ootaka T (1986) Vascularized periosteal grafts: an experimental study using two different forms of tibial periosteum in rabbits. Plast Reconstr Surg 78: 489-497.

16. Takato T, Harii K, Nakatsuka T (1988) Osteogenic capacity of vascularised periosteum: experimental study using rib periosteum in rabbits. Br J Plast Surg 41: 528-532.

17. Uddströmer L, Ritsila V (1978) Osteogenic capacity of periosteal grafts. A qualitative and quantitative study of membranous and tubular bone periosteum in young rabbits. Scand J Plast Reconstr Surg 12: 207-214.

18. Uddströmer L, Ritsila V (1979) Healing of membranous and long bone defects. An experimental study in growing rabbits. Scand J Plast Reconstr Surg 13: 281-287.

19. Oni OO, Gregg PJ (1991) An investigation of the contribution of the extraosseous tissues to the diaphyseal fracture callus using a rabbit tibial fracture model. J Orthop Trauma 5: 480-484.

20. Oni OO, Stafford H, Gregg PJ (1992) A study of diaphyseal fracture repair using tissue isolation techniques. Injury 23: 467-470.

21. Li M, Amizuka N, Oda K, Tokunaga K, Ito T, Takeuchi K, Takagi R, Maeda T (2004) Histochemical evidence of the initial chondrogenesis and osteogenesis in the periosteum of a rib fractured model: implications of osteocyte involvement in periosteal chondrogenesis. Microsc Res Tech 64: 330-342.

22. Taylor GI, Miller GD, Ham FJ (1975) The free vascularized bone graft. A clinical extension of microvascular techniques. Plast Reconstr Surg 55: 533-544.

23. Hidalgo DA (1989) Fibula free flap: a new method of mandible reconstruction. Plast Reconstr Surg 84: 71-79.

24. Chakkalakal DA, Strates BS, Mashoof AA, Garvin KL, Novak JR, Fritz ED, Mollner TJ, McGuire MH (1999) Repair of segmental bone defects in the rat: an experimental model of human fracture healing. Bone 25: 321-332.

25. Kirchen ME, O'Connor KM, Gruber HE, Sweeney JR, Fras IA, Stover SJ, Sarmiento A, Marshall GJ (1995) Effects of microgravity on bone healing in a rat fibular osteotomy model. Clin Orthop Relat Res 318: 231-242.

26. Bluhm AE, Laskin DM (1995) The effect of polyterafluoroethylene cylinders on osteogenesis in rat fibular defects: A preliminary study, J Oral Maxillofac Surg, 53: 163-166.

27. Lazard ZW, Heggeness MH, Hipp JA, Sonnet C, Fuentes AS, Nistal RP, Davis AR, Olabisi RM, West JL, Olmsted-Davis EA (2011) Cell-based gene therapy for repair of critical size defects in the rat fibula. J Cell Biochem 112: 1563-1571.

28. Arita K, Saito I, Arai Y (2006) Evaluation of mouse gutter shaped root(s) as a quantitative trait using micro-CT. Pediatr Dent J 16: 23-27.

29. Osuga N, Yang J, Yamakawa Y, Ninomiya T, Arai Y, Raorao W (2006) Micro-CT observation of rat dental pulp healing after pulpotomy in in vivo study. Pediatr Dent J 16: 132-137.

30. Saito T, Mashimo T, Shiratsuchi H, Namaki S, Matsumoto K, Mori Y, Ogasawara T, Arai Y, Honda K, Yonehara Y (2012) Evaluation of regenerative process in a rat model of mandibular condyle defect using in vivo micro x-ray computed tomography. J Hard Tissue Biol 21: 407-414.

31. Choi YS, Noh SE, Lim SM, Lee CW, Kim CS, Im MW, Lee MH, Kim DI (2008) Multipotency and growth characteristic of periosteum-derived progenitor cells for chondrogenic, osteogenic, and adipogenic differentiation. Biotechnol Lett 30: 593-601.

32. De Bari C, Dell'Accio F, Vanlauwe J, Eyckmans J, Khan IM, Archer CW, Jones EA, McGonagle D, Mitsiadis TA, Pitzalis C, Luyten FP (2006) Mesenchymal multipotency of adult human periosteal cells demonstrated by single-cell lineage analysis. Arthritis Rheum 54: 1209-1221.

33. Nakahara H, Dennis JE, Bruder SP, Haynesworth SE, Lennon DP, Caplan AI (1991) In vitro differentiation of bone and hypertrophic cartilage from periosteal-derived cells. Exp Cell Res 195: 492-503.

34. Nakahara H, Bruder SP, Goldberg VM, Caplan AI (1990) In vivo osteochondrogenic potential of cultured cells derived from the periosteum. Clin Orthop Relat Res 259: 223-232.

35. Augello A, Kurth TB, De Bari C (2010) Mesenchymal stem cells: a perspective from in vitro cultures to in vivo migration and niches. Eur Cell Mater 20: 121-133.

36. Pittenger MF, Mackay AM, Beck SC (1999) Multilineage potential of adult human mesenchymal stem cells. Science 284: 143-147.

37. Huja SS, Beck FM (2008) Bone remodeling in maxilla, mandible, and femur of young dogs. Anat Rec 291: 1-5.

38. Rockwood CA, Green DP (1975) Fractures. JB Lippincott, Philadelphia: 98-100.

39. Fujii T, Ueno T, Kagawa T, Sakata Y, Sugahara T (2006) Comparison of bone formation in grafted periosteum harvested from tibia and calvaria. Microsc Res Tech 69: 580-584.

40. Mashimo T, Saito T, Shiratsuchi H, Namaki S, Matsumoto K, Mori Y, Arai Y, Honda K, Yonehara Y (2013) Assessment of the bone regenerative process from fibular periosteum by in vivo micro computed tomography. J Hard Tissue Biol 22: 391-400.

41. Ishida H, Tamai S, Yajima H, Inoue K, Ohgushi H, Dohi Y (1996) Histologic and biochemical analysis of osteogenic capacity of vascularized periosteum. Plast Reconstr Surg 97: 512-518.

42. Vögelin E, Jones NF, Lieberman JR, Baker JM, Tsingotjidou AS, Brekke JH (2002) Prefabrication of bone by use of a vascularized periosteal flap and bone morphogenetic protein. Plast Reconstr Surg 109: 190-198.

43. Groger A, Klaring S, Merten H, Holste J, Kaps C, Sittinger M (2003) Tissue engineering of bone for mandibular augmentation in immunocompetent minipig: preliminary study. Scand J Plast Reconstr Surg Hand Surg 37: 129-133.

44. Weiland AJ, Phillips TW, Randolph MA. Bone grafts: a radiologic, histologic, and biomechanical model comparing autografts, allografts, and free vascularized bone grafts (1984) Plast Reconstr Surg 74: 368-379.

45. Chen NT, Glowacki J, Bucky LP, Hong HZ, Kim WK, Yaremchuk MJ. The roles of revascularization and resorption on endurance of craniofacial onlay bone grafts in the rabbit (1994) Plast Reconstr Surg 93: 714-722.

46. Buchman SR, Ozaki W. The ultrastructure and resorptive pattern of cancellous onlay bone grafts in the craniofacial skeleton (1999) Ann Plast Surg 43: 49-56.

47. Iwata M, Nishijima K. Experimental study of two-step grafting of fetal bone: comparison with newborn bone and influence of MHC (1994) Transplant Proc 26: 959-962.

48. Iwata M, Nishijima K (1997) Possible use of fetal bone as two-step bone grafting material-Part 2: antigenicity of fetal bone and time suitable for fetal bone grafting. Transplant Proc 29: 2283-2287.

49. Leapman SB, Deutsch AA, Grand RJ, Folkman J (1974) Transplantation of fetal intestine: survival and function in a subcutaneous location in adult animals. Ann Surg 179: 109-114.

50. Barakat TI, Harrison RG (1971) The capacity of fetal and neonatal renal tissues to regenerate and differentiate in a heterotopic allogeneic subcutaneous tissue site in the rat. J Anat 110: 393-407.

51. Spence RK, Perloff LJ, Barker CF (1979) Fetal pancreas in treatment of experimental diabetes in rats. Transplant Proc 11: 533-536.

52. Touraine JL (1979) Human T-lymphocyte differentiation in immunodeficiency diseases and after reconstitution by bone marrow or fetal thymus transplantation. Clin Immunol Immunopathol 12: 228-237.

53. Madrazo I, Drucker-Colín R, Díaz V, Martínez-Mata J, Torres C, Becerril JJ (1987) Open microsurgical autograft of adrenal medulla to the right caudate nucleus in two patients with intractable Parkinson's disease. N Engl J Med 316: 831-834.

54. Lindvall O, Brundin P, Widner H, Rehncrona S, Gustavii B, Frackowiak R, Leenders KL, Sawle G, Rothwell JC, Marsden CD (1990) Grafts of fetal dopamine neurons survive and improve motor function in Parkinson's disease. Science 247: 574-577.

55. Brown J, Clark WR, Makoff RK, Weisman H, Kemp JA, Mullen Y (1978) Pancreas transplantation for diabetes mellitus. Ann Intern Med 89: 951-965.

56. Meyer U, Wiesmann HP, Berr K, Kübler NR, Handschel J (2006) Cell-based bone reconstruction therapies-principles of clinical approaches. Int J Oral Maxillofac Implants 21: 899-906.

57. Drosse I, Volkmer E, Capanna R, De Biase P, Mutschler W, Schieker M (2008) Tissue engineering for bone defect healing: an update on a multi-component approach. Injury 39 Suppl 2: S9-20.

58. Zins JE, Whitaker LA (1983) Membranous versus endochondral bone: implications for craniofacial reconstruction. Plast Reconstr Surg 72: 778-785.

59. Donos N, Kostopoulos L, Tonetti M, Karring T (2005) Long-term stability of autogenous bone grafts following combined application with guided bone regeneration. Clin Oral Implants Res 16: 133-139.

Tables and Figures

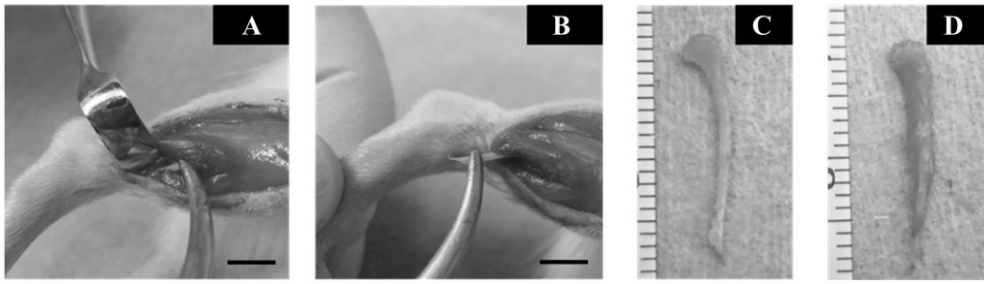

Fig. 1. Intraoperative images

A: The epiphysis of the fibula was held by surgical clips. (scale bar: 5 mm); B: The fibula was pulled out in the peripheral direction with the surgical clips. (scale bar: 5 mm); C: The removed fibula with the periosteum preserved in the PP model. (18 mm in length); D: The removed fibula with the periosteum removed in the PR model. (18 mm in length)

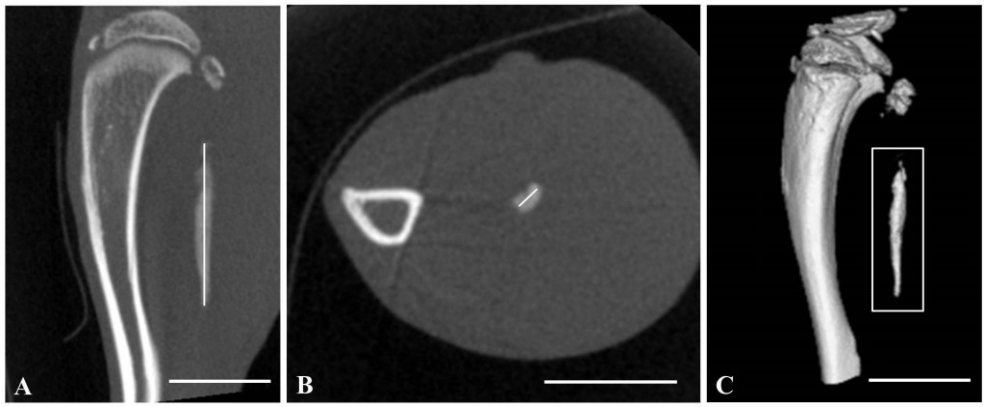

Fig. 2. Measurement of regenerative bone

A: The line indicates the longest length of regenerative bone in the longitudinal plane images. (scale bar: 5 mm); B: The line indicates the longest diameter of regenerative bone in the cross-sectional plane images. (scale bar: 5 mm); C: The square indicates the measuring range of regenerative bone volume and mineral density. (scale bar: 5 mm)

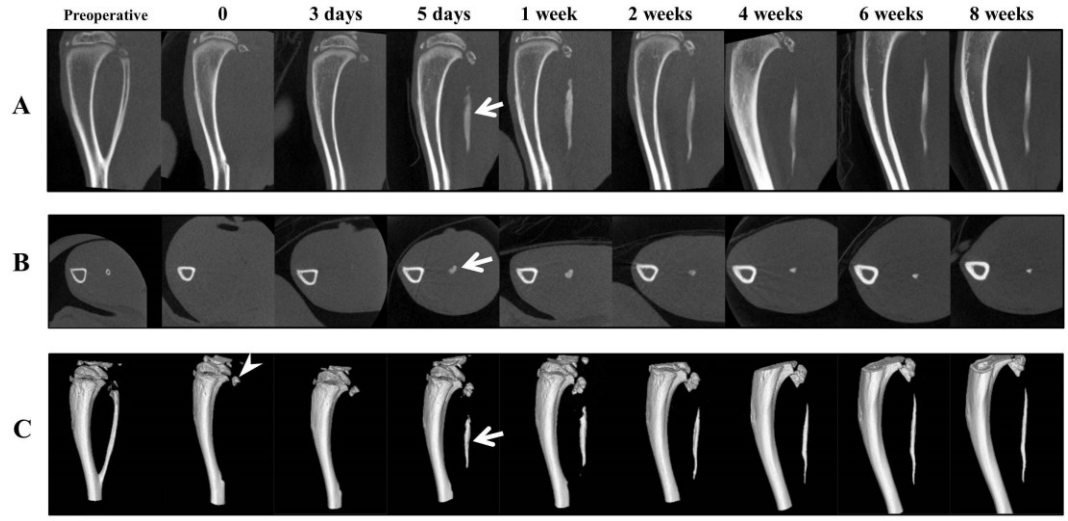

Fig. 3. CT images in the PP model

A: Longitudinal plane images are shown. The arrow indicates the regenerative bone; B: Cross-sectional plane images are shown. The arrow indicates the regenerative bone; C: Three-dimensional (3D) images are shown. The arrow indicates the regenerative bone, and the arrowhead indicates the articular cartilage.

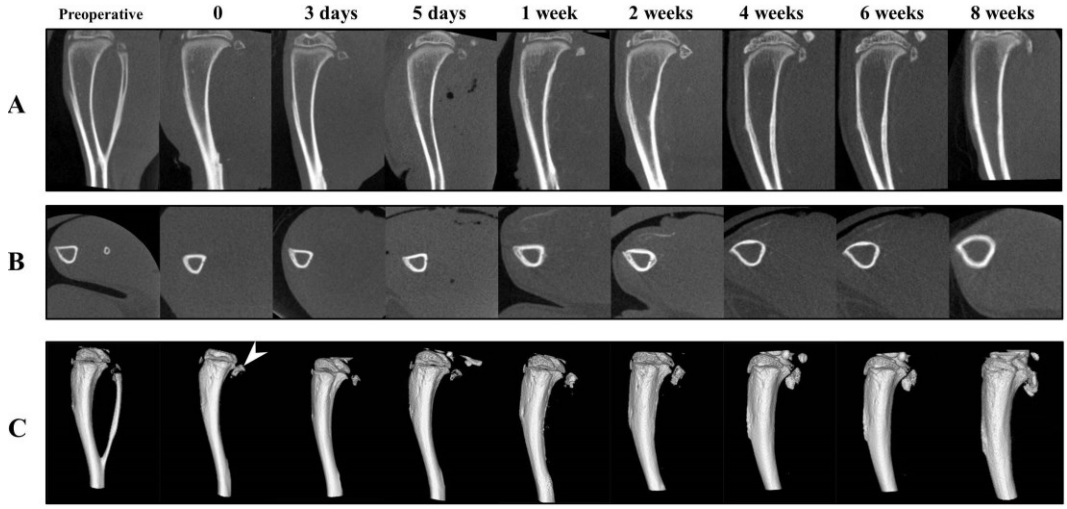

Fig. 4. CT images of the PR model

A: Longitudinal plane images are shown. No regenerative bone was observed; B: Cross-sectional plane images are shown. No regenerative bone was observed; C: Three-dimensional (3D) images are shown. No regenerative bone was observed, but the articular cartilage was evident (arrowhead).

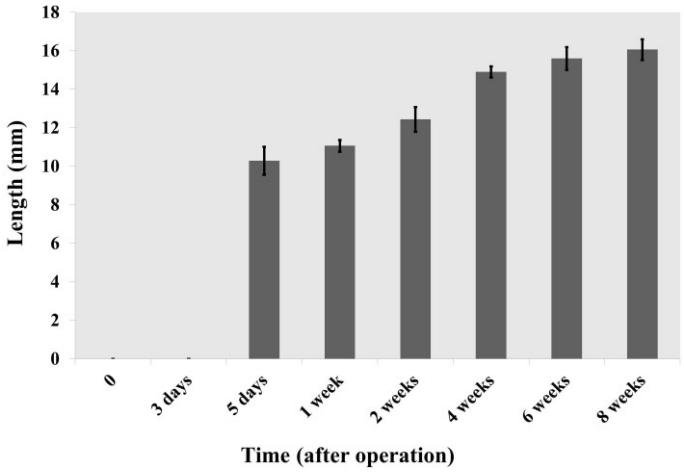

Fig. 5. Time course of the length of the regenerative bone

The length tended to increase gradually until 8 weeks. Each bar indicates the mean ± SD of five independent experiments.

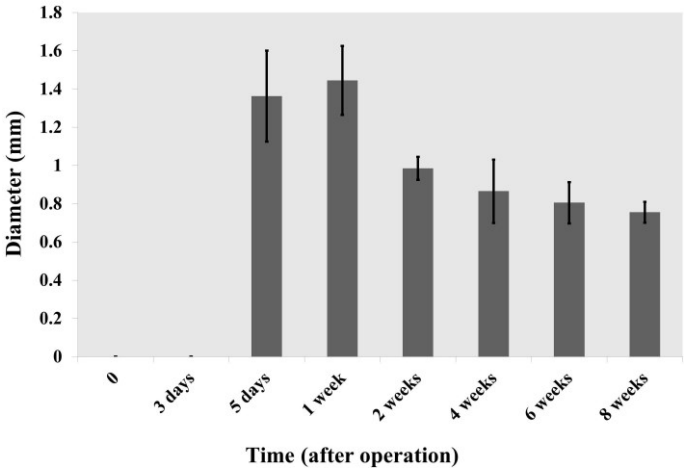

Fig. 6. Time course of the diameter of the regenerative bone

The diameter of the cross-sectional image was thickest at 1 week, but then gradually decreased. Each bar indicates the mean ± SD of five independent experiments.

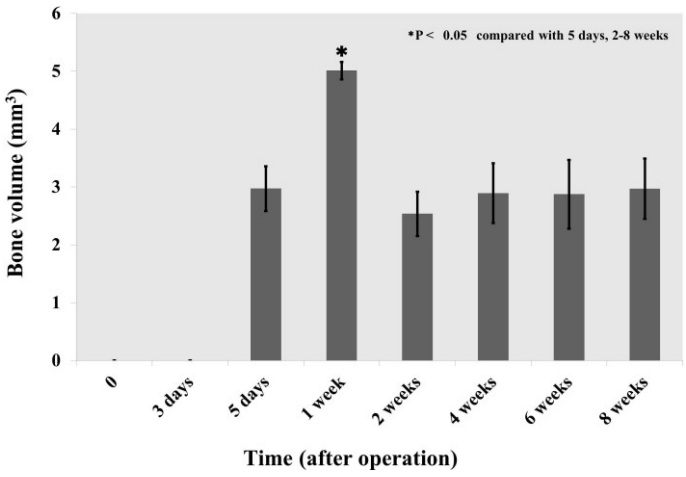

Fig. 7. Time course of regenerative bone volume

Bone volume increased remarkably at 1 week ($P < 0.05$), but decreased at 2 weeks. After 2 weeks, bone volume increased slightly up to 4 weeks. Little change was seen from 4 weeks to 8 weeks. Each bar indicates the mean ± SD of five independent experiments.

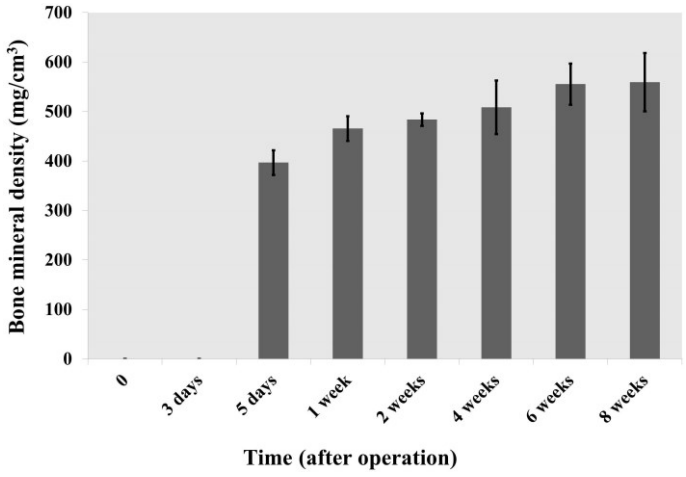

Fig. 8. Time course of regenerative bone mineral density

Bone mineral density continued to increase gradually up to 6 weeks. There was little change between 6 and 8 weeks. Each bar indicates the mean ± SD of five independent experiments.

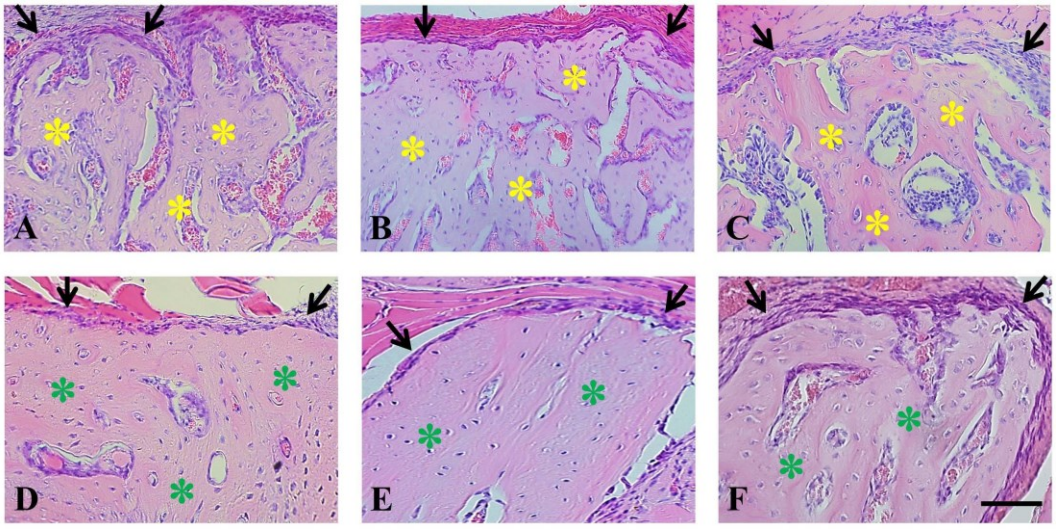

Fig. 9. The section at the center of regenerative bone in the PP model

A: 5 days after operation; B: 1 week after operation; C: 2 weeks after operation; D: 4 weeks after operation; E: 6 weeks after operation; F: 8 weeks after operation; (Hematoxylin-eosin staining, 200-fold magnification, cross sections, scale bar: 100 μm. Black arrow: periosteum. Yellow asterisk: woven bone. Green asterisk: lamellar bone.)

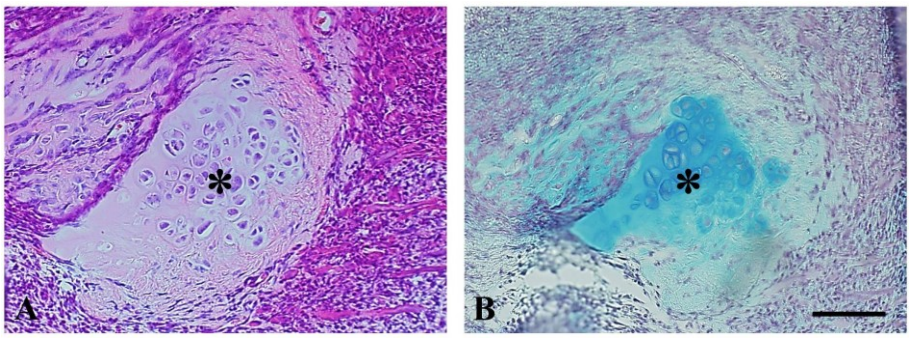

Fig. 10. The section at the epiphysis of regenerative bone in the PP model (5 days)

A: Hematoxylin-eosin staining, 200-fold magnification, cross sections, scale bar: 100 μm (black asterisk: cartilage-like tissue); B: Alcian blue staining, 200-fold magnification, cross sections, scale bar: 100 μm; (black asterisk: cartilage-like tissue)

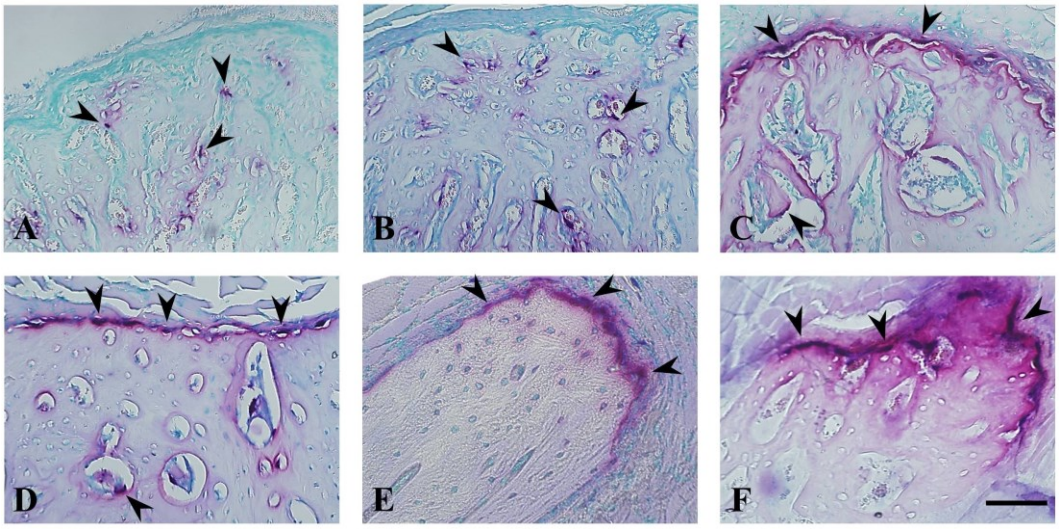

Fig. 11. TRAP staining of the section at the center of regenerative bone in the PP model

A: 5 days after operation; B: 1 week after operation; C: 2 weeks after operation; D: 4 weeks after operation; E: 6 weeks after operation; F: 8 weeks after operation; (200-fold magnification, cross sections, scale bar: 100 μm. Black arrowhead: $TRAP^{+}$ osteoclast)

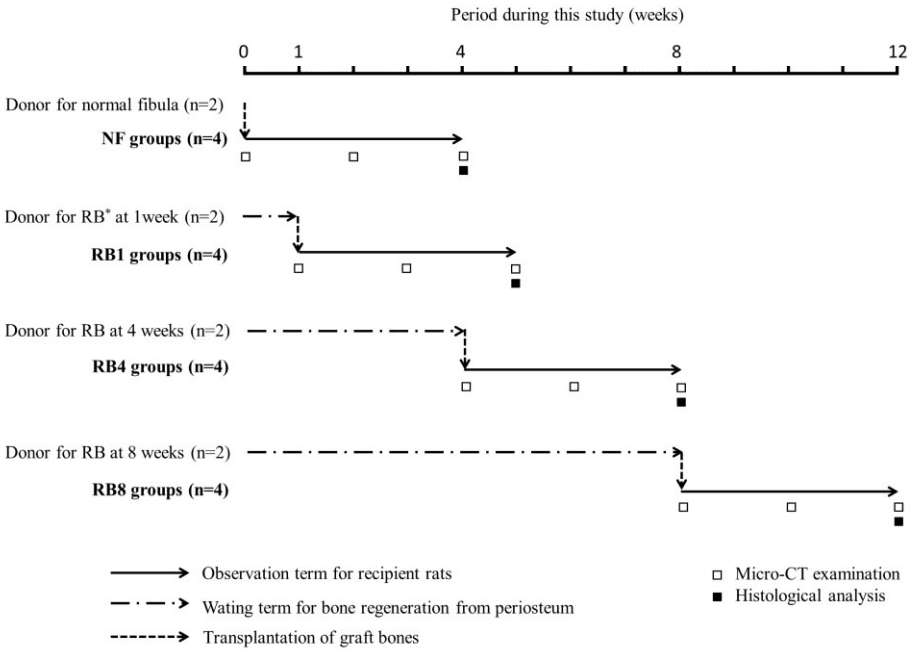

Fig. 12. Experimental protocol

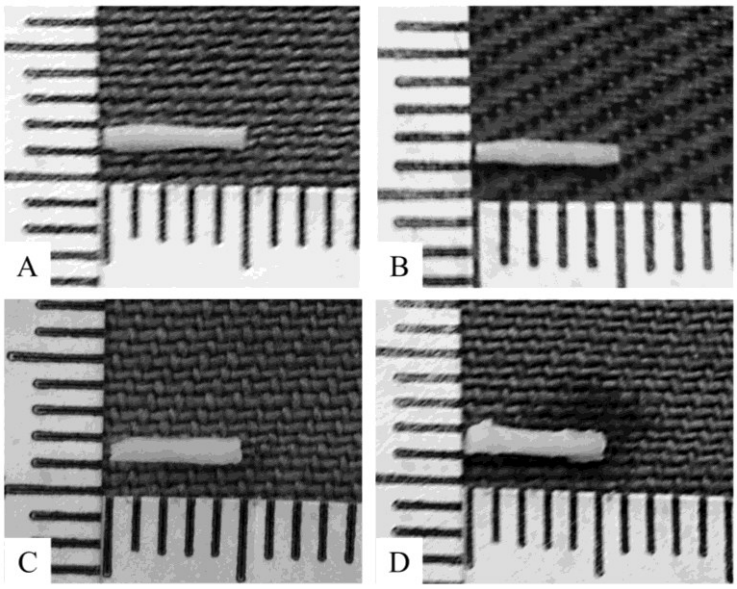

Fig. 13. Each graft bone after trimming

A: normal fibula; B: regenerative bone at 1 week; C: regenerative bone at 4 weeks; D: regenerative bone at 8 weeks (size = 1×5 mm).

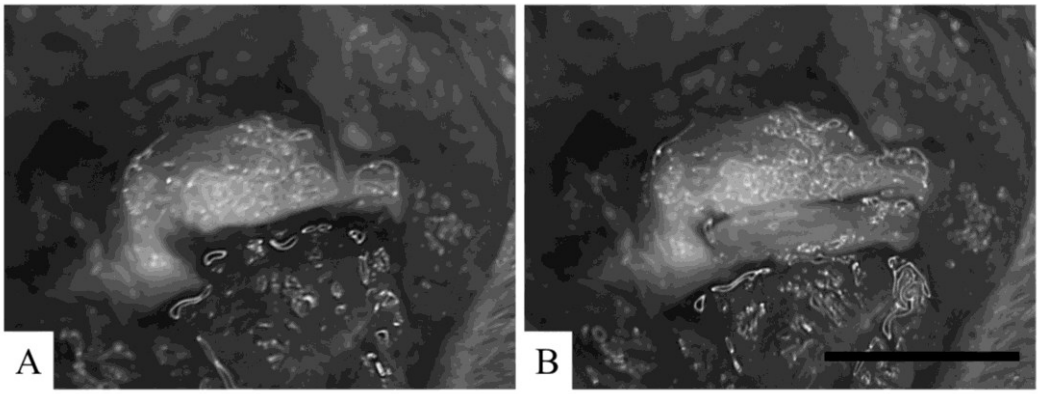

Fig. 14. Intraoperative images

A: A bone defect was made at the mandibular inferior border (scale bar = 5 mm); B: The graft bone was transplanted into the bone defect (scale bar = 5 mm).

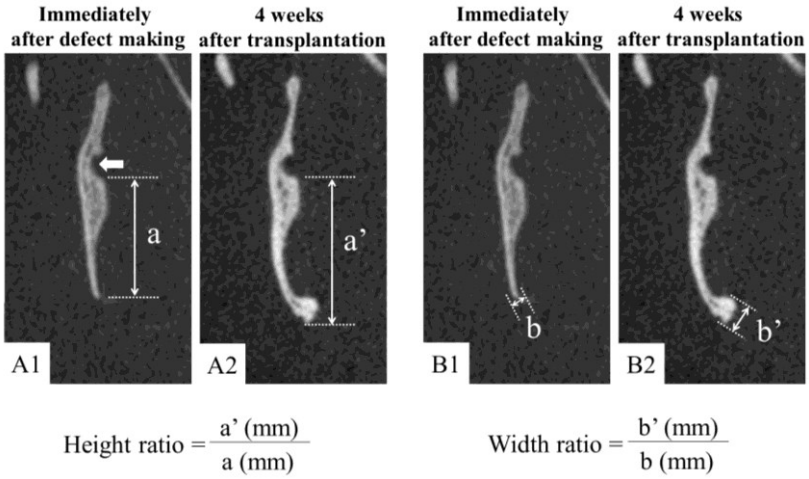

Fig. 15. Measurement of the height and width of the mandible using image reconstruction software

A-1: "a " indicates the height immediately after making the defect; A-2: "a' " indicates the height after 4 weeks; B-1: "b " indicates the width immediately after making the defect; B-2: "b' " indicates the height after 4 weeks.

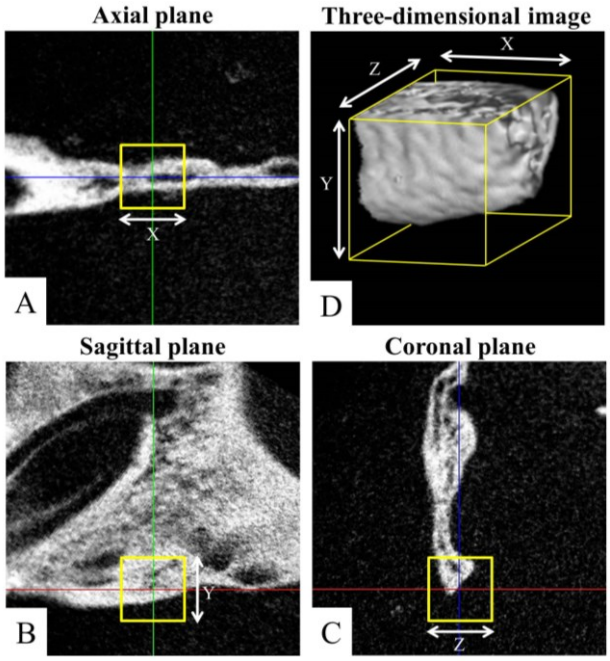

Fig. 16. Measurement of the bone mineral density in the rectangle using quantitative analysis software

A: Axial plane is shown (X = 2 mm); B: Sagittal plane is shown (Y = 2 mm); C: Coronal plane is shown (Z = 2 mm); D: Three-dimensional image is shown. The rectangle range (2 × 2 × 2 mm) is measured.

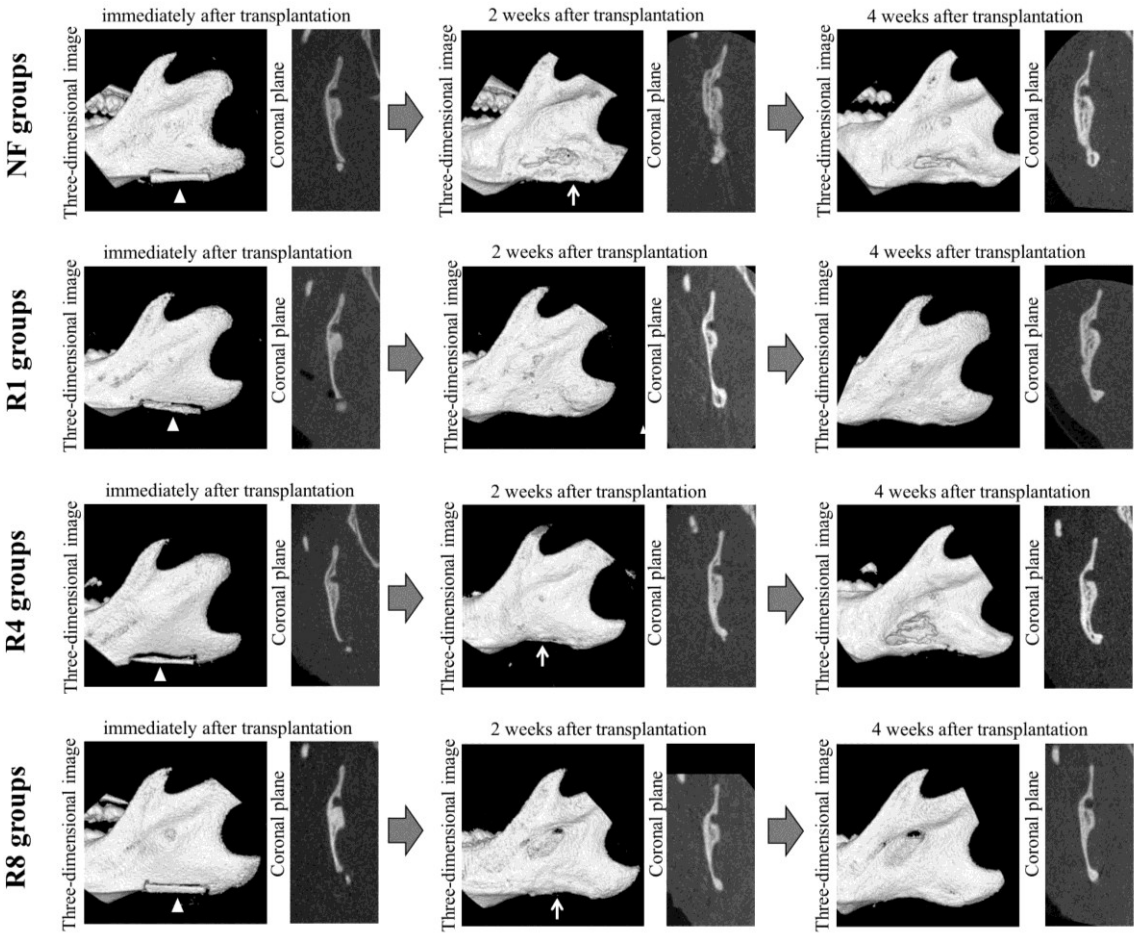

Fig. 17. Micro-CT images showing each group immediately, 2 and 4 weeks after transplantation

Arrowheads indicate graft bone immediately after transplantation. Arrows indicate resorbed graft bone 2 weeks after transplantation.

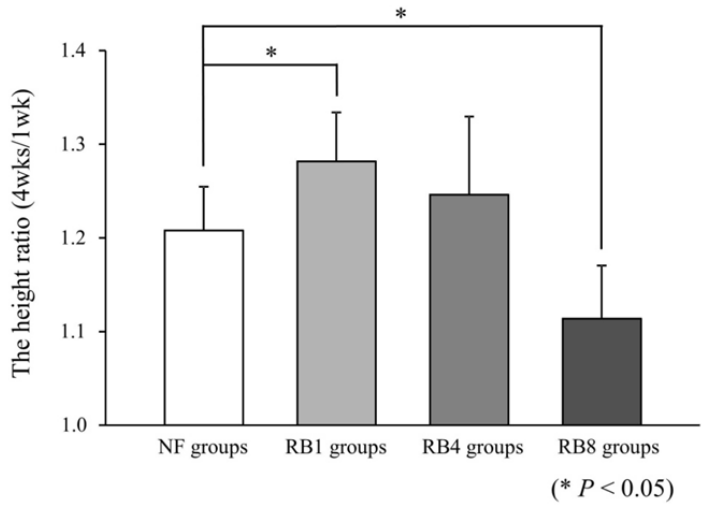

Fig. 18. The height ratio (height 4 weeks after transplantation/height immediately after defect making)

Each bar indicates the mean ± SD of four independent experiments. * $P < 0.05$, compared with the NF groups.

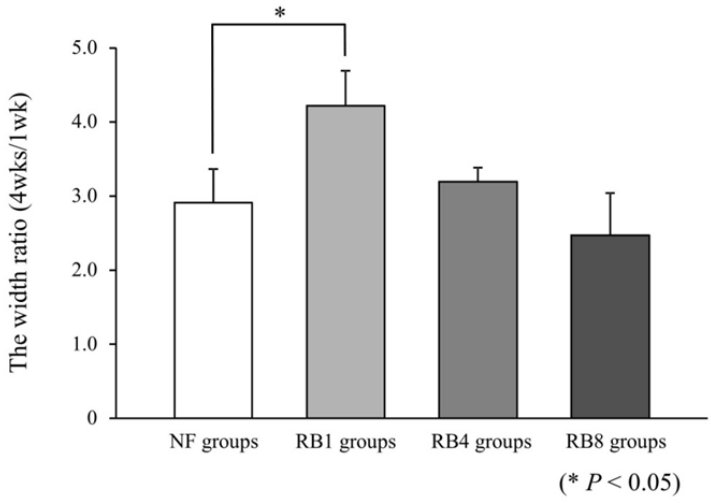

Fig. 19. The width ratio (width 4 weeks after transplantation/width immediately after defect making)

Each bar indicates the mean ± SD of four independent experiments. * $P < 0.05$, compared with the NF groups.

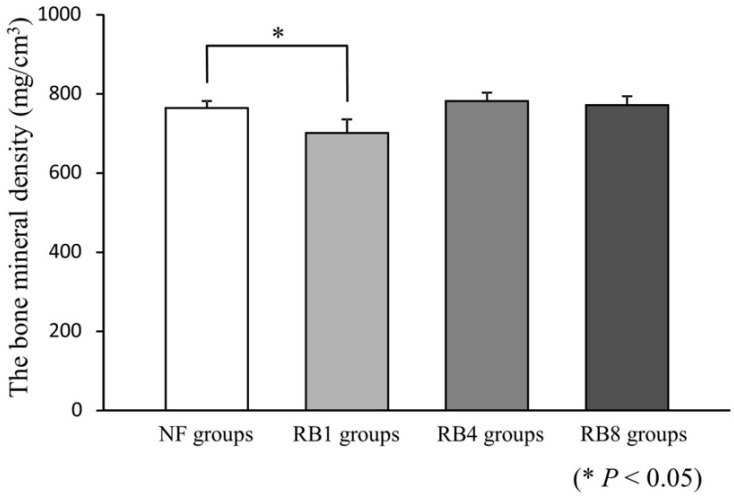

Fig. 20. The bone mineral density 4 weeks after transplantation

Each bar indicates the mean ± SD of four independent experiments. * $P < 0.05$, compared with the NF groups.

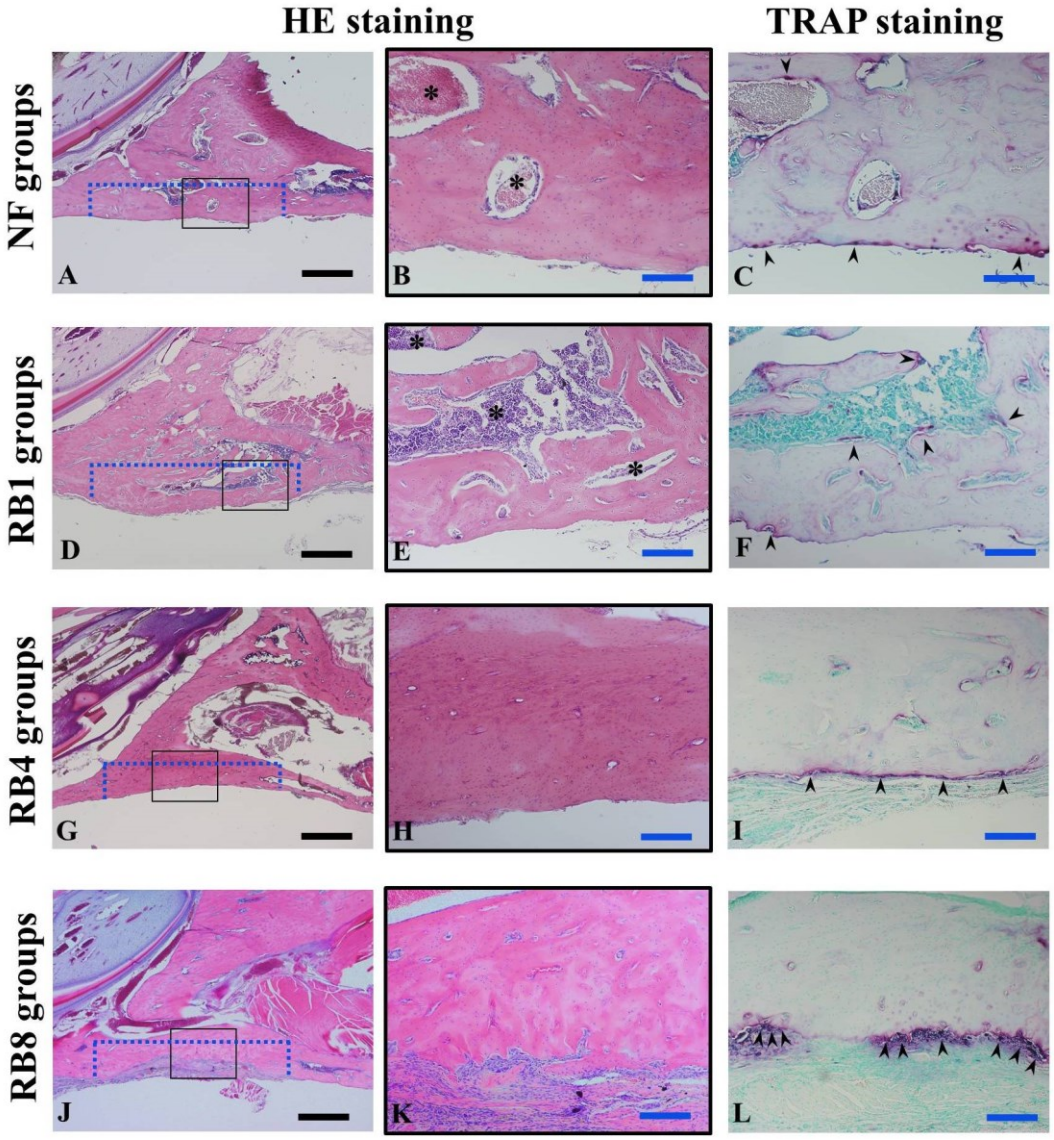

Fig. 21. Sagittal sections of the bone graft site in the mandible 4 weeks after transplantation

A-C: NF groups (A and B are HE staining. C is TRAP staining.); D-F: R1 groups (D and E are HE staining. F is TRAP staining.); G-I: R4 groups (G and H are HE staining. I is TRAP staining.); J-L: R8 groups (J and K are HE staining. L is TRAP staining.); Blue dotted lines indicate the bone defect. Black asterisks indicate bone marrow. Black arrowheads indicate $TRAP^{+}$ osteoclasts. Black scale bar = 1000 μm. Blue scale bar = 200 μm.

Table. Mean of each measurements in the regenerative bone

The mean ± SD of five independent experiments